

TERNARY PHASE EQUILIBRIA IN TRANSITION METAL-
BORON-CARBON-SILICON SYSTEMS

Part I. Related Binary Systems
Volume VIII. Zr-B System

E. Rudy
St. Windisch

*** Export controls have been removed ***

~~This document is subject to special export controls and each transmittal to foreign governments or foreign nationals may be made only with prior approval of Metals and Ceramics Division, Air Force Materials Laboratory, Wright-Patterson Air Force Base, Ohio.~~ *This document has been approved for public release and sale; its distribution is unlimited.*

FOREWORD

The work described in this report was carried out at the Materials Research Laboratory, Aerojet-General Corporation, Sacramento, California, under USAF Contract No. AF 33(615)-1249. The contract was initiated under Project No. 7350, Task No. 735001. The program is administered under the direction of the Air Force Materials Laboratory Research and Technology Division, with Captain R. A. Peterson and Lt. P.J. Marchiando acting as Project Engineers and Dr. E. Rudy, Aerojet-General Corporation, as Principal Investigator. Professor Dr. H. Nowotny, University of Vienna, served as consultant to the project.

The project, which includes the experimental and theoretical investigation of related binary and ternary systems in the system classes Me_1 - Me_2 -C, Me-B-C, Me_1 - Me_2 -B, Me-Si-B, and Me-Si-C, was initiated on 1 January 1964.

The phase diagram work was performed by E. Rudy and St. Windisch. Assisting in the investigations were: J. Pomodoro (preparation of sample material), T. Eckert (DTA-runs), J. Hoffman (metallographic preparations), and R. Cobb (X-ray exposures).

Chemical analysis of the alloys was performed under the supervision of Mr. W. E. Trahan, Quality Control Division of Aerojet-General Corporation. The authors wish to thank Mr. R. Cristoni for the preparation of the illustrations and Mrs. J. Weidner, who typed the report.

The manuscript of this report was released by the authors October 1965 for publication as an RTD Technical Report.

Other reports issued under USAF Contract AF 33(615)-1249 have included:

Part I. Related Binaries

Volume I. Mo-C System

Volume II, Ti-C and Zr-C Systems

Volume III, Systems Mo-B and W-B

Volume IV, Hf-C System

Volume V, Ta-C System. Partial Investigations in the Systems V-C and Nb-C

Volume VI, W-C System. Supplemental Information on the Mo-C System

Volume VII, Ti-B System

Contrails

FOREWORD (Cont'd)

Part II. Ternary Systems

Volume I. Ta-Hf-C System

Volume II, Ti-Ta-C System

Volume III, Zr-Ta-C Systems

Volume IV, Ti-Zr-C, Ti-Hf-C, and Zr-Hf-C Systems

Part III. Special Experimental Techniques

Volume I, High Temperature Differential Thermal
Analysis

Part IV. Thermochemical Calculations

Volume I, Thermodynamic Properties of Group IV,
V, and VI Transition Metal Carbides

This technical report has been reviewed and is approved.



W. G. RAMKE

Chief, Ceramics and Graphite Branch
Metals and Ceramics Division
Air Force Materials Laboratory

ABSTRACT

The binary alloy system zirconium-boron has been investigated by means of X-ray, metallographic, melting point, and differential-thermo-analytical techniques. The experimental alloy material comprised of hot-pressed and heat-treated, arc- and electron-beam melted, as well as equilibrated and quenched alloy material. All phases of the experimental investigations were supported by chemical analysis.

The results of the present investigation, which resulted in the establishment of a complete phase diagram for the system, are discussed and compared with previously established system data.

TABLE OF CONTENTS

	PAGE
I. INTRODUCTION AND SUMMARY.	1
A. Introduction	1
B. Summary	1
II. LITERATURE REVIEW.	4
III. EXPERIMENTAL PROGRAM.	7
A. Sample Preparation and Experimental Procedures.	7
1. Starting Materials.	7
2. Specimen Preparation and Heat Treatment.	9
3. Differential Thermal Analysis.	10
4. Melting Point Determinations.	10
5. X-Ray Investigations.	11
6. Chemical Analysis.	11
7. Metallographic Procedures.	12
B. Results	12
1. The Zirconium Phase.	12
2. The Concentration Range Zr to ZrB ₂	13
3. The Diboride Phase	21
4. Boron-Rich Equilibria	25
IV. DISCUSSION	33
References	34

ILLUSTRATIONS

FIGURE		PAGE
1	Constitution Diagram Zirconium-Boron	3
2	Phase Diagram Zirconium-Boron (F. W. Glaser and B. Post, 1953; W. Schedler, 1951, Work Quoted by R. Kieffer and F. Benesovsky, 1963)	4
3	Zr-B (1.8 At% B), Quenched with $\sim 80^\circ\text{C}$ per Second from 1790°C	13
4	DTA-Thermograms (Cooling) of Crystal-Bar Zirconium and a Zirconium-Boron Alloy with 6 Atomic Percent Boron	14
5	Zr-B (50 At% B) with 3 At% Carbon Added	15
6	Zr-B (50 At% B), with 8 At% Carbon Added	15
7	Melting Temperatures and Solid State Reaction Isotherms in the Zirconium-Boron System	16
8	DTA-Thermogram of a Zirconium-Boron Alloy with 50 Atomic Percent Boron	17
9	Zr-B (5 At% B), Quenched from 1740°C	20
10	Zr-B (11 At% B), Quenched from 1700°C	20
11	Zr-B (14 At% B), Quenched with $\sim 80^\circ\text{C}$ per Second from 1700°C	21
12	Lattice Parameters of ZrB_2 as a Function of the Boron Concentration.	22
13	Zr-B (64.8 At% B), Quenched from 2000°C	22
14	Zr-B (65.4 At% B), Quenched from 2600°C	23
15	Zr-B (65.8 At% B), Quenched from 3000°C	23
16	Zr-B (66.2 At% B), Quenched from 3245°C	24
17	Zr-B (68.3 At% B), Quenched from 2700°C	24
18	DTA-Thermogram (Cooling) of a Zirconium-Boron Alloy with 80 Atomic Percent Boron	26
19	DTA-Thermogram of the Alloy from Figure 18 (80 At.% B) at Lower Heating and Cooling Rates	27

ILLUSTRATIONS (Continued)

FIGURE		PAGE
20	DTA-Thermogram of a Zirconium-Boron Alloy with 95 Atomic Percent Boron	28
21	Zr-B (80 At% B), Cooled with Approximately 20°C per Second from 2280°	29
22	Zr-B (80 At% B), Partially Melted at 2280°C, Re-annealed at 2200°C, and Quenched	29
23	Zr-B (88 At% B), Melted, Re-equilibrated at 2200°C, and Quenched	30
24	Zr-B (90 At% B), Cooled with ~ 10°C per Second from 2200°C	30
25	Zr-B (90 At% B), Alloy from Figure 24 Re-equilibrated for 1/2 Hour at 2200°C, and Quenched	31
26	Zr-B (87 At% B), Melted, Re-equilibrated at 2200°C, and Cooled with 2°C per Second	31
27	Zr-B (99 At% B), Cooled with Approximately 10°C per Second from 2100°C.	32

TABLES

TABLES		PAGE
1	Isothermal Reactions in the System Zirconium-Boron	3
2	Structure and Lattice Parameters of Zirconium Borides	6
3	Reported Melting Temperatures for Zirconium-Boron Alloys	7
4	Melting Temperatures of Zirconium-Boron Alloys, and Qualitative Phase Evaluation	18

I. INTRODUCTION AND SUMMARY

A. INTRODUCTION

In continuation of our work on the high-temperature phase relationships in binary and ternary systems of the refractory transition metals with selected B-elements, the emphasis in the present series of investigations was directed towards the group IV metal-boron systems. The phase diagram work performed on the zirconium-boron system will be described in this report.

Like in every re-evaluative type of investigation, the present work draws heavily on the data and the experience established during previous investigations. With the main objective of the overall program being the establishment of the high temperature phase relationships in ternary systems, the reinvestigation of the corresponding binaries was carried to an extent only, as it proved to be necessary for a reliable interpretation of the ternary results.

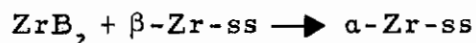
B. SUMMARY

Two intermediate phases, a congruently melting hexagonal diboride, and a peritectically decomposing dodecaboride of cubic symmetry, the latter being unstable at temperatures below 1700°C, are formed in this alloy system. The previously reported face-centered cubic monoboride does not exist as a pure binary phase.

1. The Zirconium Phase

β -zirconium melts at 1876°C. The hexagonal close-packed α -modification transforms at $872 \pm 15^\circ\text{C}$ into the body-centered cubic

(β) high temperature modification. β -Zr forms a eutectic equilibrium with the diboride (12 At% B, 1660°C), and takes at this temperature less than 1 atomic percent boron into solid solution. The α - β -transformation is slightly increased by boron additions (872°C in pure zirconium, 880°C in excess diboride-containing alloys), thus suggesting a peritectoid reaction of the type.

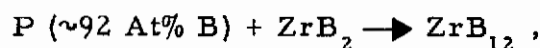


2. Zirconium Diboride

Zirconium diboride, with a hexagonal, C32 type of crystal structure ($a = 3.167 \text{ \AA}$; $c = 3.530 \text{ \AA}$) melts congruently at 3245°C at compositions close to stoichiometry. The phase has a negligible (<2 At% B) range of homogeneity.

3. Zirconium Dodecaboride (ZrB₁₂)

The pinkish-purple-colored, metallic dodecaboride occurs at slightly substoichiometric (stoichiometric = 92.3 At% B; actual: ~90-91 At% B) compositions, and has a face-centered cubic, $D2_f(UB_{12})$ -type of crystal structure, with $a = 7.408 \text{ \AA}$. The phase forms in a peritectic reaction at 2250°C from diboride and melt according to



and decomposes at 1710°C in a comparatively rapid eutectoid reaction into diboride and boron. A eutectic equilibrium (~98 At% B, 2000°C) is formed between the dodecaboride and boron.

Table 1. Isothermal Reactions in the System Zirconium-Boron

Temperature, °C	Reaction	Compositions of the Equilibrium Phases, At% B			Type of Reaction
3245°	$L \rightarrow ZrB_2$	66	66	--	Congruent Transformation
2250°	$L + ZrB_2 \rightarrow ZrB_1$	92	+66.6	~90	Peritectic Reaction
~2100	$L \rightarrow B$	100	100	--	Melting Point of Boron
2000	$L \rightarrow ZrB_{12} + B$	~98	~91	>99	Eutectic Reaction
1876°	$L \rightarrow \beta-Zr$	0	0	--	Melting Point of Zirconium
1710°	$ZrB_{12} \rightarrow ZrB_2 + B$	~90	66.6	>99	Eutectoid Reaction
1660°	$L \rightarrow \beta-Zr + ZrB_2$	12	<1	~66	Eutectic Reaction
880°	$\beta-Zr + ZrB_2 \rightarrow \alpha-Zr$	<1	~66	<<1	Peritectoid Reaction
872°	$\beta-Zr \rightarrow \alpha-Zr$	0	0	--	α - β -Transformation in Zirconium

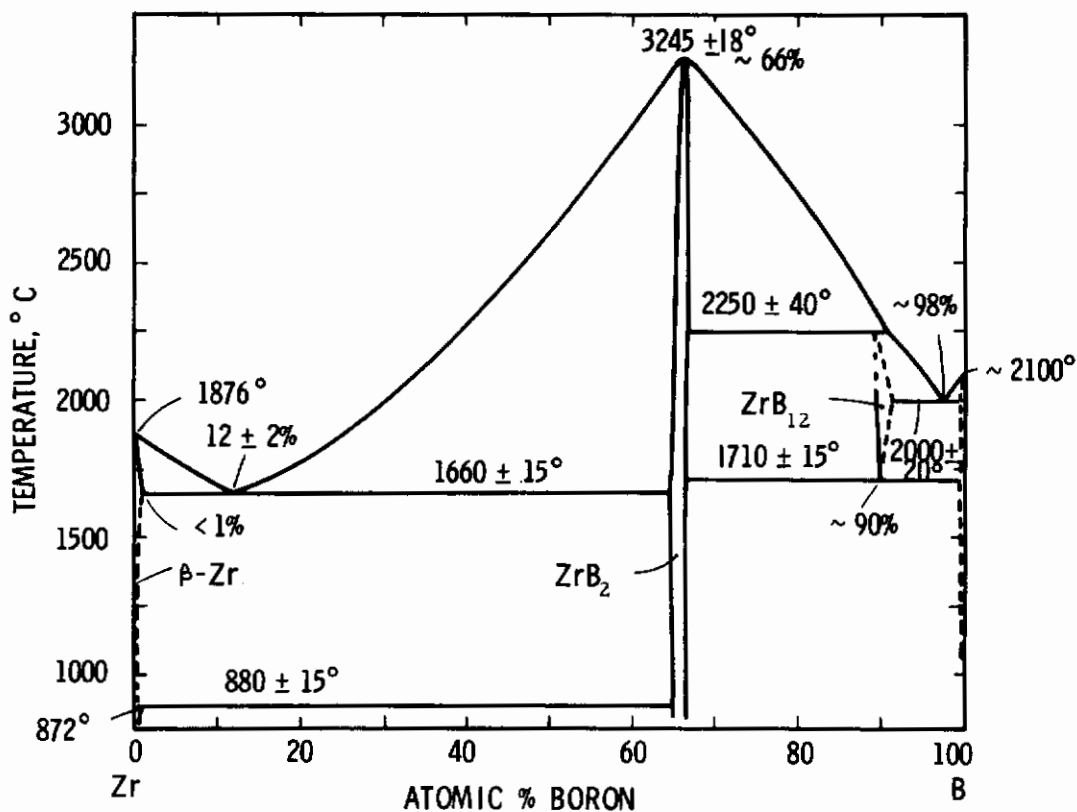


Figure 1. Constitution Diagram Zirconium-Boron

II. LITERATURE REVIEW

Two intermediate phases, a hexagonal ZrB_2 , and a face-centered cubic dodecaboride ZrB_{12} , the latter being unstable below approximately $1600^\circ C$, occur in the system. A previously claimed, face-centered cubic (B1) monoboride " ZrB "^(1, 2, 3) does not exist⁽⁴⁾.

Zirconium diboride⁽⁵⁾ has a hexagonal, C32-type of crystal structure⁽⁶⁾, with $a = 3.169 \text{ \AA}$, and $c = 3.530 \text{ \AA}$ (Table 2). The phase has a narrow range of homogeneity^(6, 7, 4).

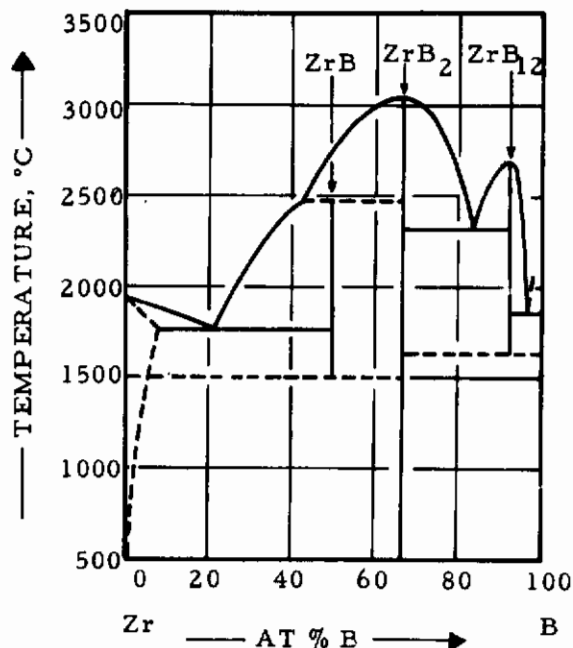


Figure 2. Phase Diagram Zirconium-Boron
(F. W. Glaser and B. Post, 1963, W. Schedler 1951;
Work Quoted by R. Kieffer and F. Benesovsky, 1963)

ZrB_{12} has a face-centered cubic, $D2_f(UB_{12})$ -type of structure, with $a = 7.408 \text{ \AA}$ ^(1, 2), and is unstable at temperatures below approximately $1600^\circ C$ ⁽³⁾.

Contrails

A monoboride ZrB , with a face-centered cubic (B1) structure, $a = 4.65 \text{ \AA}$, was said to be stable only between 800 and 1250°C ^(1, 2, 3). W. Schedler⁽⁸⁾ reports its temperature range of stability to lie between approximately 1500°C and 2400°C . The occurrence of this phase was not observed by R. Kiessling⁽⁶⁾ and other, later investigations^(7, 4), which leads one to suspect, that the previously observed 'monoboride' actually refers to impurity phases of the type $Zr(O, N, C, B)_{1-x}$. In this direction also point lattice parameter considerations, since the parameters given for this phase ($a \sim 4.65 \text{ \AA}$) generally lie between those of the binary compounds of zirconium with the corresponding impurity elements: $a_{ZrC_{1-x}} : 4.68$ to 4.60 \AA ; $a_{ZrN_{1-x}} = 4.58 \text{ \AA}$; $a_{ZrO_{1-x}} : 4.58$ to 4.62 \AA , a face-centered cubic (B1) binary monoboride would have the significantly larger parameter of $a = 4.76 \text{ \AA}$ ⁽⁴⁾.

Based on X-ray evidence, R. Kiessling⁽⁶⁾ places the solid solubility limit of boron in zirconium at approximately 1 atomic percent. According to V. A. Epelbaum and M.A. Gurewitsch⁽⁹⁾ the incorporation of boron (up to a maximum of 2 atomic percent) is accompanied by a sizeable increase of the lattice parameters of zirconium. Higher boron solubilities in zirconium found by W. Schedler⁽⁸⁾ are probably due to oxygen or nitrogen contamination of the alloys.

The high-temperature phase relationships in this alloy system were investigated by W. Schedler⁽⁸⁾ and by F. W. Glaser and B. Post⁽³⁾ (Figures 2 and 3, Table 3). Reported melting temperatures for the diboride phase vary between 3040°C (K. Moers, 1931⁽¹⁰⁾) and $\pm 50^\circ\text{C}$ (C. Agte, 1931⁽¹¹⁾). More recent determinations by F. W. Glaser and co-workers^(3, 12) are difficult to assess, since no experimental details on the techniques used were given.

Table 2. Structure and Lattice Parameters of Zirconium Borides

Phase	Structure	Lattice Parameters, Å	
		Literature Data	This Investigation
ZrB*	fcc., B1-type	a = 4.65 ± 0.03 (3)	Not confirmed
ZrB ₂	hex., C32-type (AlB ₂)	a = 3.169 c = 3.530 (6) a = 3.170 c = 3.533 (13, 14) a = 3.168 ± 0.002 c = 3.528 ± 0.002 (15) a = 3.167 c = 3.530 (4)	a = 3.167 ± 0.002 Å c = 3.530 ± 0.001 Å
ZrB ₁₂	fcc., D2 _f -type	a = 7.408 (2) a = 7.408 (4)	a = 7.408 Å

*Probably Zr (N, O, C) Solid Solution

The metal-rich eutectic was placed at approximately 22 atomic percent boron and a temperature of 1760°C^(3, 8). More recent investigations by L. Kaufmann and co-workers⁽¹³⁾ indicate somewhat lower temperatures (1500°C < T_{eut} < 1650°C).

Table 3. Reported Melting Temperatures of Zirconium-Boron Phases

Alloy	Temp °C	Compos. At% B	Investigator	Ref	Remarks
Zr-(ZrB)ZrB ₂ Eutectic	1760°	22	F.W. Glaser & B. Post (1953)	35	
			W. Schedler, 1951	41	
	1650°	n.d.	L.Kaufmann & E.V.Clougherty (1965)	45	
ZrB	2480°	~50	W. Schedler, 1951	41	peritect. decomp.
	1500°		W. Schedler, 1951	41	eutect. decomp.
	1250°		F.W.Glaser & B.Post (1953)	35	peritect. decomp.
	800°		F.W.Glaser & B.Post (1953)		eutectoid decomp
	2350°		L.Kaufmann, et.al. (1965)	45	peritect. decomp.
ZrB ₂	3190±50	66	C. Agte (1931)	44	congruent melt.
	3040°		K. Moers, (1931)	43	
			F.W.Glaser & B.Post (1953)	35	
ZrB ₁₂	2680°	90-92	W. Schedler (1951)	41	congruent melt.
			F.W.Glaser & B.Post (1953)	35	

III. EXPERIMENTAL PROGRAM

A. SAMPLE PREPARATION AND EXPERIMENTAL PROCEDURES

1. Starting Materials

The powdered elements as well as zirconium dihydride and zirconium diboride were employed for the preparation of the experimental alloys.

Zirconium and zirconium dihydride were purchased in powdered form from Wah Chang Corporation, Albany, Oregon. The zirconium powder had the following impurities (contents in ppm): C-40, Fe-315, Hf-67, O-839,

Contrails

Ta-<400, sum of other impurities-<460. The particle size of the powder was between 44 and 74 μ , and lattice parameters of $a = 3.232 \text{ \AA}$, and $c = 5.149 \text{ \AA}$ were measured from an X-ray exposure with copper- K_{α} radiation.

The analysis supplied for zirconium dihydride (2.1 Wt% H) was (contents in ppm) C-320, Cu-125, Fe-1800, Hf-137, Mg-255, N-116, O-1300, Si-157, Ta-<200, sum of others-<405.

The boron powder with a purity of 99.55% was purchased from United Mineral and Chemical Corporation, New York. Major impurities were iron (0.25%) and carbon (0.1%).

Zirconium diboride was prepared by direct combination of the elements at high temperatures. In order to eliminate difficulties arising from the violent reaction, a master alloy containing 85 atomic percent boron was initially prepared. After comminution, this intermediate reaction product was intimately mixed with the necessary amount of zirconium and cold-compacted. The green compacts were then loaded into a tantalum container and reacted for approximately two hours at temperatures between 1800° and 2000°C under a high purity helium atmosphere. After cooling under vacuum, the zones which were in contact with the tantalum container were scraped off, and the reaction lumps precrushed to pellets of approximately 2 millimeters in diameter. Comminution to the desired grain sizes of <60 micrometers was achieved by ball-milling in hard-metal lined jars. Cobalt traces picked up during the grinding process, were removed by a leaching treatment in a boiling 8N mixture of hydrochloric and sulfuric acid. The acid-powder slurry was then filtered and washed with water until the filtrate was neutral, the major portion of the water removed by acetone and ether, and the powder dried under vacuum. The chemical analysis of the diboride gave a boron

content of 65.2 At% B; it also contained 0.11 Wt% carbon. A semiquantitative spectrographic analysis gave the following additional impurity contents (in ppm): Fe-<300, Si-100, Mg-<100, Al-<100, Ca-<100, Co-not detected, Cu, Ni, Mn-<100, Cr-not detected, Mo-<100, Ti-200, V, W, Ta-not detected. X-ray diffraction showed only the diboride ($a = 3.167 \text{ \AA}$; $c = 3.530 \text{ \AA}$), while the metallographic analysis indicated the presence of small quantities of excess metal phase.

2. Specimen Preparation and Heat Treatment

A total of 73 alloy samples were prepared for melting point, DTA, as well as X-ray studies on solid state equilibrated samples.

High-boron (>70 AtT) alloys were prepared by hot-pressing, while metal-rich alloy mixtures were cold-pressed and sintered. A number of compositions were arc melted prior to homogenization, and selected samples from the very metal-rich (<15 At% C), specifically intended for melting point and DTA-studies were electron-beam molten (Heraeus gun ES-2/4) under a vacuum of better than 10^{-5} Torr.

The homogenization treatments were carried out in a tungsten-mesh element furnace manufactured by the R. Brew Company under a high purity helium atmosphere. The tantalum sample container was wrapped in zirconium foil, in order to reduce the pick-up of impurity traces from the furnace atmosphere to a minimum. Main equilibration temperature for the investigations of the solid state portion of the system was 1400°C (80 hours); equilibration studies of higher temperatures were carried out in the Pirani-furnace, and the samples were quenched in tin.

Approximately one-fourth of the experimental sample material, mostly with compositions around the diboride and dodecaboride, were subjected to chemical analysis for boron, and selected excess-metal containing

samples were spot-checked for interstitial impurities, such as oxygen and nitrogen. In general, good concentration stability with regard to the weighed-in compositions was observed, and the oxygen and nitrogen contents of the alloys after the runs were at a negligible (<200 ppm) level.

3. Differential Thermal Analysis

Apparative details of the DTA setup have been described in earlier reports^(16, 17). For alloys with boron contents below 60 atomic percent the measurements were carried out under vacuum, while diboride and excess boron-containing alloys were run under 1.5 atmospheres of helium. To retard interaction between the sample and the graphite containers, linings of tantalum as well as zirconium diboride were employed for the high temperature runs. The situation, however, remained unsatisfactory, since the lack of adequate container materials limited the DTA-investigations to temperatures below 2500°C.

4. Melting Point Determinations

Melting temperatures of the alloys were determined using the previously described⁽¹⁶⁾ Pirani-technique. A small sample bar with dimensions varying from 4 x 4 mm to 10 x 10 mm cross section and from 20 to 40 mm in length, is heated resistively to the temperature of the phase change. The temperature of the sample is measured optically with a disappearing filament type pyrometer through a quartz window mounted in the furnace wall. A small hole, generally in the order of 0.6 mm in diameter, pressed or drilled into the sample, serves as the reference point for the measurements.

The overall uncertainties in the temperature are composed of two-parts: The precision of the measurements, and the errors in the pyrometer calibrations. They can be computed for the relation:

$$\bar{\sigma} = + \sqrt{\sigma_c^2 + \sigma_m^2}$$

where $\bar{\sigma}$ stands for the overall temperature uncertainty, σ_c for the standard deviation in the pyrometer calibration in the given temperature range, and σ_m denoting the precision of the measurement. Typical calibration uncertainties are $\pm 10^\circ\text{C}$ at 2300°C , $\pm \sim 17^\circ\text{C}$ at 3000°C , and $\pm 30^\circ\text{C}$ (estimated) at 4000°C .

The temperature figures in the text and on the figures refer to the precision of the measurements, since it was felt, that these data are more representative of the relative accuracy attained in the experiments.

5. X-Ray Investigations

X-ray powder patterns with Cu-K_α radiation were prepared from all samples prepared during the course of the investigations. Excess zirconium alloys were difficult to crush, and the powders had to be stress-annealed prior to the exposures. The X-ray exposures were made in a 57.4 mm diameter camera on a Siemens Crystalloflex II unit, and the diffraction patterns were measured on a Siemens Kirem coincidence scale with precision micrometer attachment.

6. Chemical Analysis

The principle of the wet chemical method used for the boron determinations consists in converting the boron contained in the alloy to boric acid, which then is determined by differential titration on the complex acid formed with mannitol. The detailed procedures were analogously to those for the titanium-boron system, described in a previous report⁽¹⁸⁾.

The carbon content of the alloys was determined using the standard combustion technique; for carbon contents below 0.1 Wt% the gas analysis was performed conductometrically, Oxygen and nitrogen were analysed for in a high temperature ($\sim 2300^{\circ}\text{C}$) gas fusion analyzer, and small impurity contents were determined in a semiquantitative way spectrographically.

7. Metallographic Procedures

The specimens were mounted in an electrically conductive combination of diallyl-phtalate and lucite-coated copper powder and coarse-ground on silicon carbide papers with grit sizes varying between 120 and 600. Polishing was done on a nylon cloth, using a slurry of 0.05 micrometer alumina and Murakami's solution.

Alloy samples with boron contents from 0 to 67 atomic percent were electroetched in a 2 N sodium hydroxide solution, which left the metal phase light-blue in appearance, while the diboride phase remained essentially unchanged. Single phase diboride alloys were etched in a 10% solution of Aqua Regia and hydrofluoric acid, whereas excess boron-containing alloys were examined in the as-polished state.

B. RESULTS

1. The Zirconium Phase

The melting point of zirconium was determined on cold-pressed as well as electron-beam molten samples, resulting in a value of $1876 \pm 4^{\circ}\text{C}$. This result was independently confirmed by a DTA-run on crystal-bar zirconium (Wah Chang Corporation), which yielded $1877 \pm 20^{\circ}\text{C}$ ⁽¹⁹⁾. The solubility of boron in β -zirconium at the eutectic temperature must be

less than one atomic percent, since an alloy with an analyzed boron content of 1.8 atomic percent already shows appreciable quantities of excess diboride (Figure 3). A small boron solubility is also indicated from the DTA-curves on low-boron alloys, which show a very small increase in the temperature of the α - β -transformation temperature as compared to pure zirconium (Figure 4).



Figure 3. Zr-B (1.8 At% B), Quenched with $\sim 80^{\circ}\text{C}$ per Second from 1790°C .

X500

Primary β -Zirconium (Transformed), and Zr + ZrB₂ Eutectic.

2. The Concentration Range Zr to ZrB₂

Alloys with boron concentrations varying from 2 to 65 atomic percent are two-phased containing the metal and diboride phase in varying amounts. In a number of alloys the presence of barely detectable

quantities of B1-phase was noticed on the X-ray films. From the analytical results, correlated with the metallographic and X-ray evidence gained on ternary Zr-B-C alloys, which show a steady increase of the amount of B1-phase with increasing carbon content (Figure 5 and 6), the appearance of the face-centered cubic phase is definitely related to the presence of carbon impurities⁽²⁰⁾. The same behavior also is indicated by the incipient melting temperatures of the alloys (Figure 7 and 8, Table 4), which coincide over the entire concentration range under discussion with the temperature of the metal-rich eutectic (1660°C). In the average, lattice parameters of $a = 3.23_8 \text{ \AA}$, and $c = 5.16_2 \text{ \AA}$ were measured for the zirconium phase in excess diboride containing alloys, which are slightly higher than those of the starting material, ($a = 3.232 \text{ \AA}$; $c = 5.149 \text{ \AA}$).

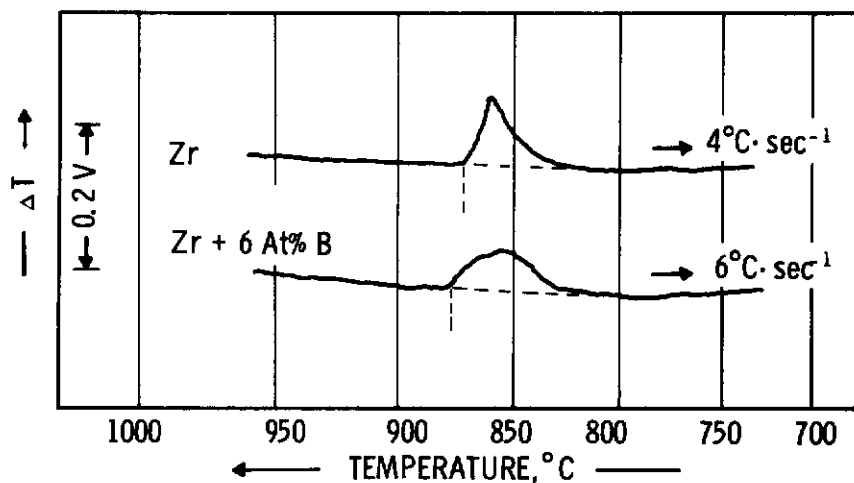


Figure 4. DTA-Thermograms (Cooling) of Crystal-Bar Zirconium and a Zirconium-Boron Alloy with 6 Atomic Percent Boron.

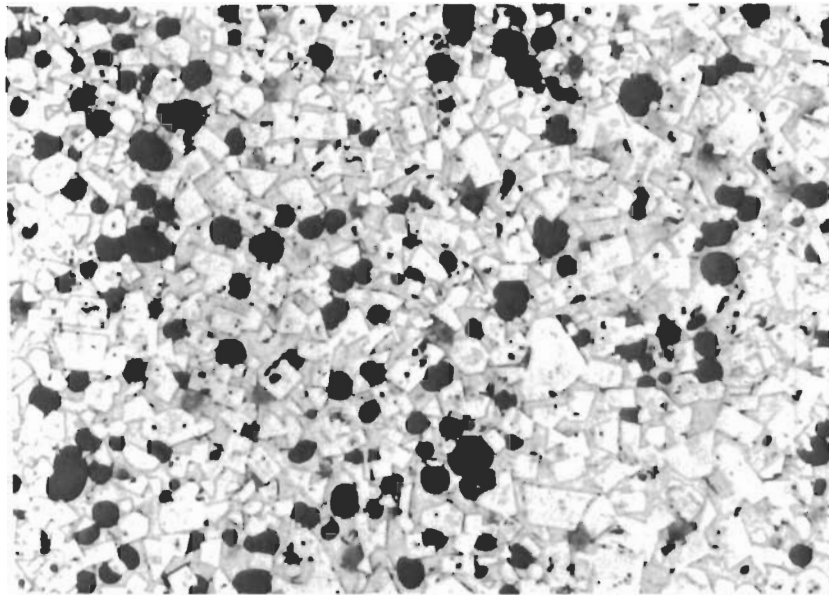


Figure 5. Zr-B (50 At% B), with 3 At% Carbon Added Alloy Quenched from 1800°C.

X400

Zr-ZrB₂, and Dark Round Crystals of Zirconium Monocarbide Solid Solution. $a_{\text{ZrC-ss}} = 4.676 \text{ \AA}$.

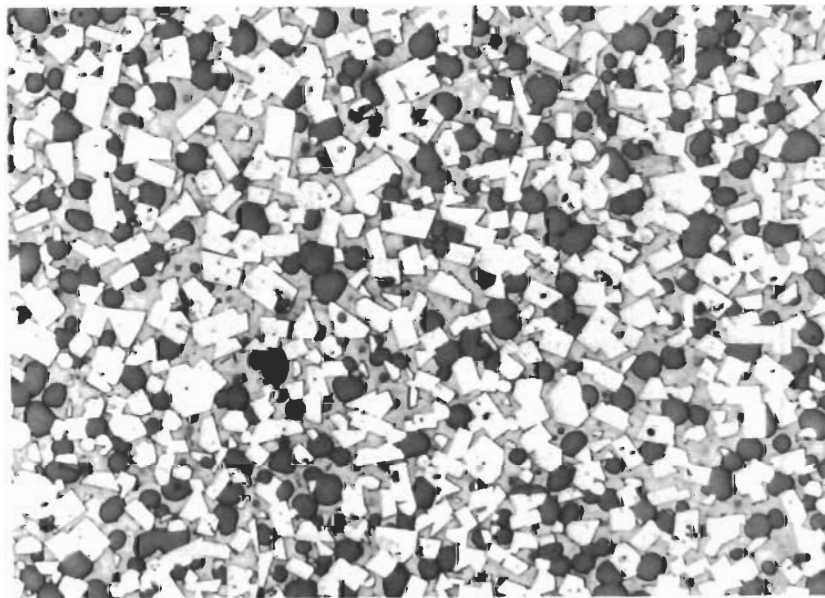


Figure 6. Zr-B (50 At% B), with 8 At% Carbon Added Alloy Quenched from 1800°C.

X400

Increasing Amounts of ZrC-ss (Round, Dark Crystals) in a Base Alloy Consisting of Zr and ZrB₂.

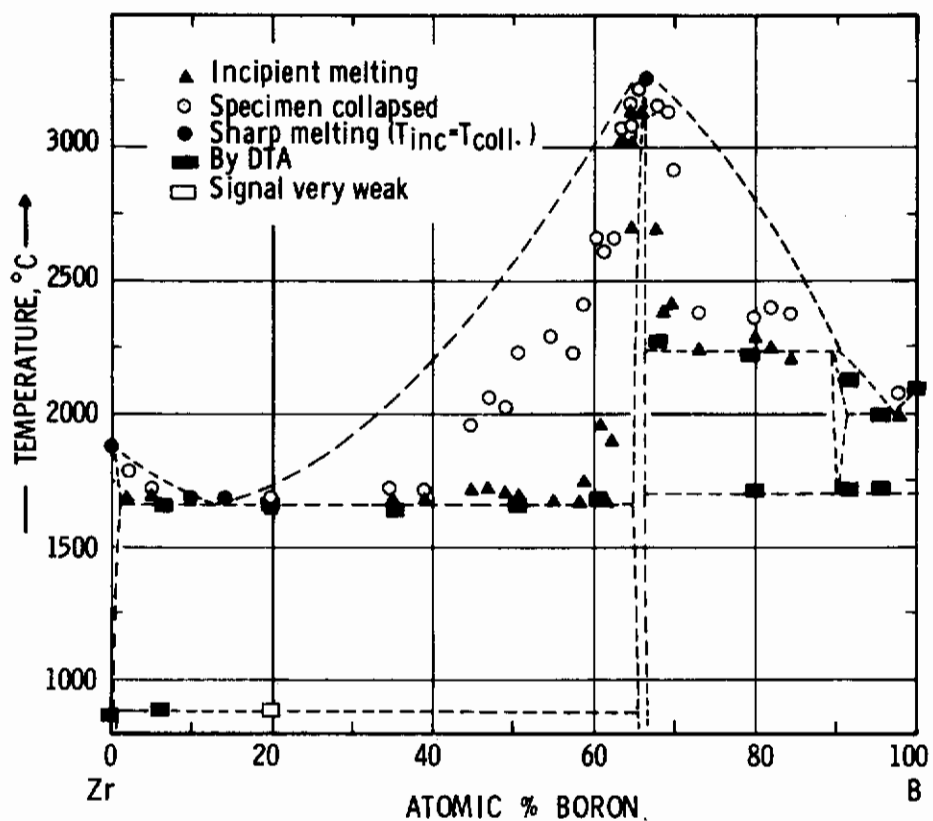


Figure 7. Melting Temperatures and Solid State Reaction Isotherms in the Zirconium-Boron System

The eutectic point was located at 12 At% B by inspecting metallographically samples which had been quenched from temperatures above the eutectic line (Figures 9 through 11). Similar to the observations in the titanium-boron system⁽¹⁸⁾, rapid quenching proved to be essential for retaining the eutectic structure, since the diboride grains tend to segregate and agglomerate extremely fast at the grain boundaries of the metal phase.

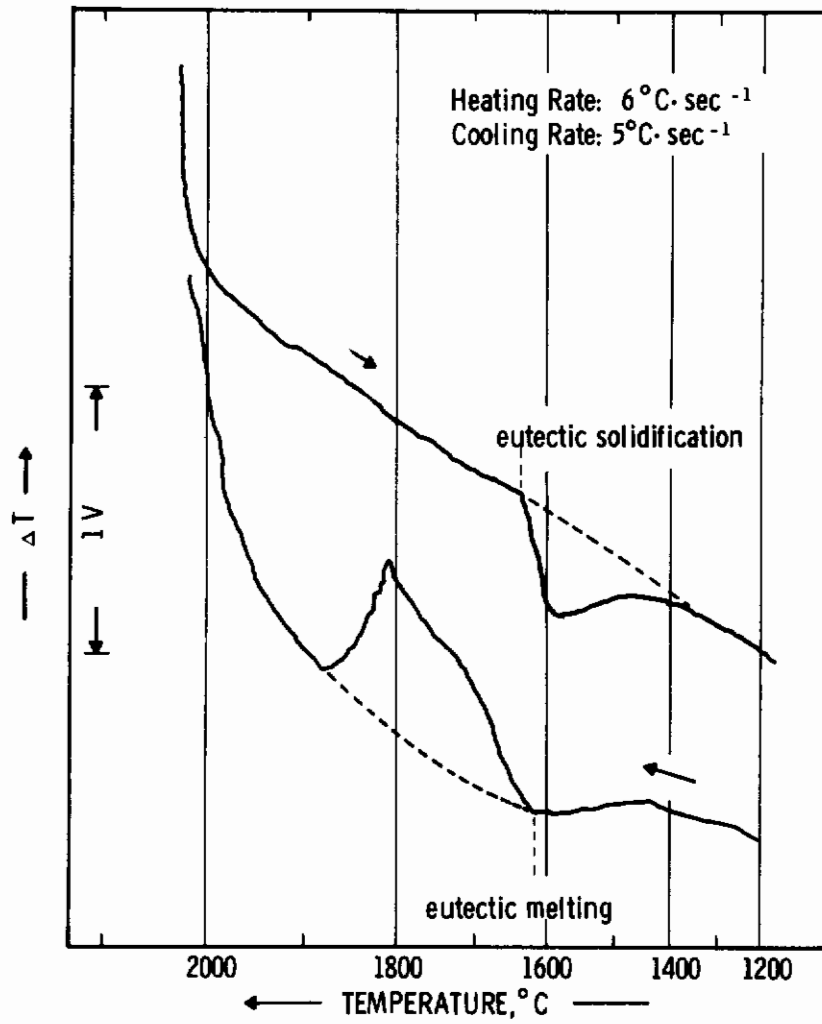


Figure 8. DTA-Thermogram of a Zirconium-Boron Alloy with 50 Atomic Percent Boron.

Table 4. Melting Temperatures of Zirconium-Boron Alloys and Qualitative Phase Evaluation

No.		Melting Temp.		Melting	Phases	X-Ray		Metallography
		Incipient °C	°C Collapse			Lattice Parameters, Å		
1	0	n.d.	1876+4°	Sharp	n.d.	n.d.	Single Phase Zr	
2	2	1.8	1705°	Heterog	n.d.	n.d.	Zr+(Zr-ZrB ₂)Eutect	
3	5	4.6	1712°	Heterog	n.d.	n.d.	Zr+(Zr+ZrB ₂)Eutect	
4	10	n.d.	1672°	Fairly Sharp	Zr + ZrB ₂	Zr:a=3.23 ₈ Å; c=5.162 ₈ Å	Zr+(Zr+ZrB ₂)Eutect	
5	15	n.d.	1668°	Fairly Sharp	Zr + ZrB ₂	n.d.	ZrB ₂ +(Zr+ZrB ₂)Eutect	
6	20	n.d.	1658°	Sl. Heterog	Zr + ZrB ₂	Zr:a=3.23 ₆ Å; c=5.17 ₄ Å	ZrB ₂ +(Zr+ZrB ₂)Eutect	
7	25	n.d.	~1683°	Heterog	Zr+ZrB ₂ +Trace B1	B1:a=4.62 ₈ Å	ZrB ₂ +Zr+B1	
8	30	n.d.	~1694°	Heterog	Zr + ZrB ₂	n.d.	Zr+ZrB ₂ +Trace B1	
9	35	n.d.	1694°	Heterog	Zr + ZrB ₂	n.d.	Zr+ZrB ₂	
10	40	39	1685°	Heterog	Zr+ZrB ₂ +Trace B1	n.d.	Zr+ZrB ₂ +Trace B1	
11	45	45	1733°	Heterog	Zr + ZrB ₂	n.d.	Zr+ZrB ₂	
12	48	47.5	1738°	Heterog	Zr + ZrB ₂	n.d.	n.d.	
13	50	49.5	1693°	Heterog	Zr + ZrB ₂	n.d.	Zr+ZrB ₂ +Trace B1	
14	52	50.3	1678°	Heterog	Zr + ZrB ₂	n.d.	Zr+ZrB ₂	
15	55	55	1674°	Heterog	Zr + ZrB ₂	n.d.	Zr+ZrB ₂	
16	58	56.4	1665°	Heterog	Zr + ZrB ₂	ZrB ₂ :a=3.167 ₈ Å; c=3.53 ₀ Å	Zr+ZrB ₂	
17	60	58.4	1740°	Heterog	Zr + ZrB ₂	n.d.	n.d.	
18	61	n.d.	1690°	Heterog	Zr + ZrB ₂	n.d.	n.d.	
19	62	60.5	1920°	Heterog	Zr + ZrB ₂	n.d.	n.d.	
20	63	n.d.	1860°	Heterog	Zr + ZrB ₂	ZrB ₂ :a=3.166 ₈ Å; c=3.531 ₈ Å	ZrB ₂ +Zr	
21	64	62.5	3006°	Heterog	Zr + ZrB ₂	n.d.	ZrB ₂ +Zr	
22	65	65	3168+20°	Heterog	ZrB ₂	ZrB ₂ :a=3.166 ₈ Å; c=3.530 ₈ Å	ZrB ₂ +Zr	
23	66	65.8	3172+18°	Fairly Sharp	ZrB ₂	ZrB ₂ :a=3.165 ₈ Å; c=3.530 ₈ Å	ZrB ₂	
24	67	66.2	3245+18°	Sharp	ZrB ₂	ZrB ₂ :a=3.167 ₈ Å; c=3.532 ₈ Å	ZrB ₂	

Table 4 (continued)

No.	Nom. Anal.	Melting Temp. °C		Melting	Phases	X-Ray		Metallography
		Incipient	Collapse			Lattice Parameters, Å		
25	68	2683°	3188°	Heterog	ZrB ₂	ZrB ₂ :a=3.166Å;c=3.53Å	ZrB ₂ +Trace B	
26	69	2340°	3160°	Heterog	ZrB ₂	n. d.	ZrB ₂ +B	
27	70	2380°	2885°	Heterog	ZrB ₂	n. d.	ZrB+B+Trace ZrB ₁₂	
28	71	~2300°	~2470°	Heterog	ZrB ₂	n. d.	ZrB+B+Trace ZrB ₂	
29	73	~2280°	~2350°	Heterog	ZrB ₂ +Trace ZrB ₁₂	ZrB:a=3.167Å;c=3.53Å	ZrB ₂ +ZrB ₁₂ +B	
30	76	2250°	2370°	Heterog	ZrB + ZrB ₁₂	ZrB ₂ :a=7.406Å	ZrB ₂ +ZrB ₁₂ +B	
31	80	2290°	2355°	Heterog	ZrB ₂ + ZrB ₁₂	n. d.	ZrB ₂ +ZrB ₁₂ +B	
32	82	2253°	2375°	Heterog	ZrB ₂ + ZrB ₁₂	n. d.	ZrB ₂ +ZrB ₁₂ +B	
33	85	2243°	2363°	Heterog	ZrB ₂ + ZrB ₁₂	n. d.	ZrB ₂ +ZrB ₁₂ +B	
34	88	~2223°	~2260°	Heterog	ZrB ₂ + ZrB ₁₂	n. d.	ZrB ₂ +ZrB ₁₂ +B	
35	90	~2060°	~2080°	Heterog	ZrB ₂ + ZrB ₁₂	ZrB ₂ :a=7.408Å	ZrB ₂ +ZrB ₁₂ +B	
36	92	~2090°	~2100°	Heterog	ZrB ₂ + ZrB ₁₂	ZrB:a=7.407Å	ZrB ₂ +ZrB ₁₂ +B	
37	98	1996°	2082°	Sl. Heterog	ZrB ₁₂ + B	n. d.	ZrB ₁₂ + B	

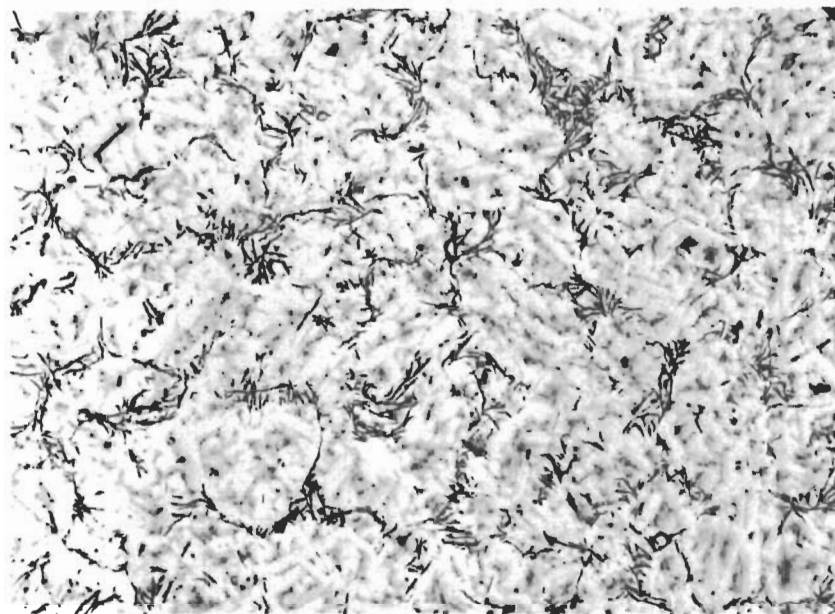


Figure 9. Zr-B (5 At% B), Tin-Quenched from 1740°C. X200
Primary β -Zirconium(Transformed), and Zr + ZrB₂ Eutectic.

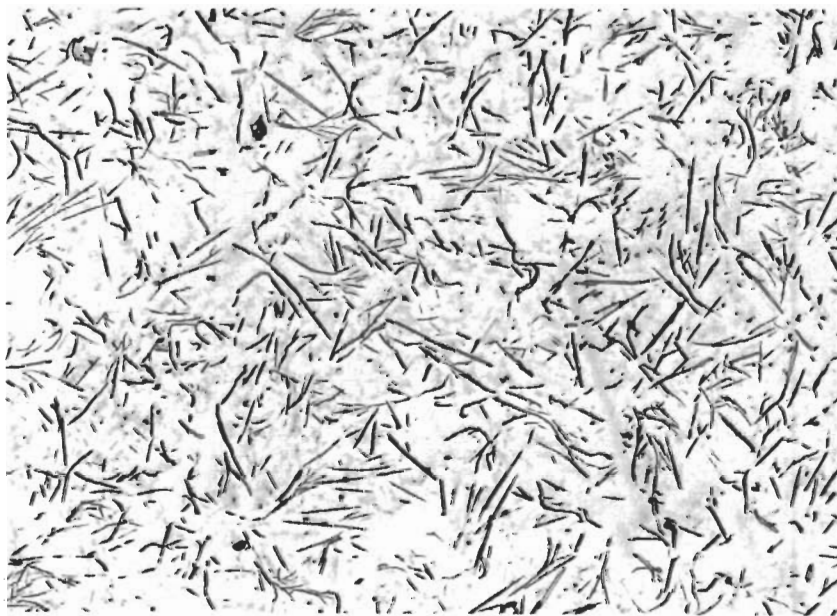


Figure 10. Zr-B (11 At% B), Tin-Quenched from 1700°C. X250
Traces of Primary β -Zirconium, and Zr + ZrB₂ Eutectic.

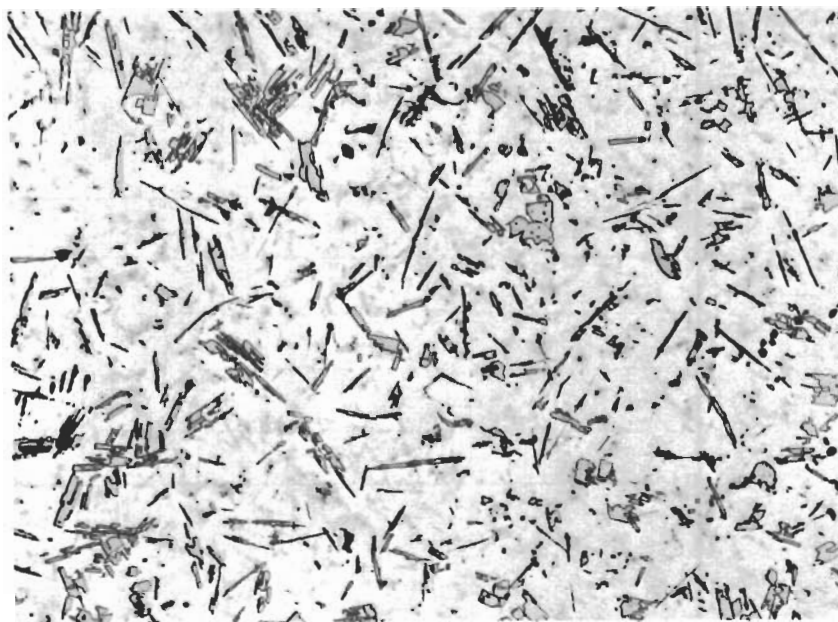


Figure 11. Zr-B (14 At% B), Quenched with $\sim 80^\circ\text{C}$ per Second X250 from 1700°C .

Partially Segregated Zr + ZrB_2 Eutectic, and Small Amounts of Primary Diboride.

3. The Diboride Phase

Although incipient melting was difficult to note in alloys above 60 atomic percent, the wide temperature gap existing between measured incipient and collapsing temperatures (Figure 7) still indicates melting to be two-phased. Congruent melting was observed to occur at 3245°C and a boron concentration of approximately 66 atomic percent. The incipient melting temperatures drop rapidly to approximately 2300°C , as the total boron content of the alloys exceeds 67 atomic percent (Table 4 and Figure 7).

The homogeneity range of the diboride is very small; within the error limits of the measurements, the same lattice parameters for ZrB_2 were measured in excess metal as well as excess ZrB_{12} -or boron-containing alloys (Figure 12). Similar conclusions were reached by metallographic inspection of quenched as well as annealed alloys, which show the

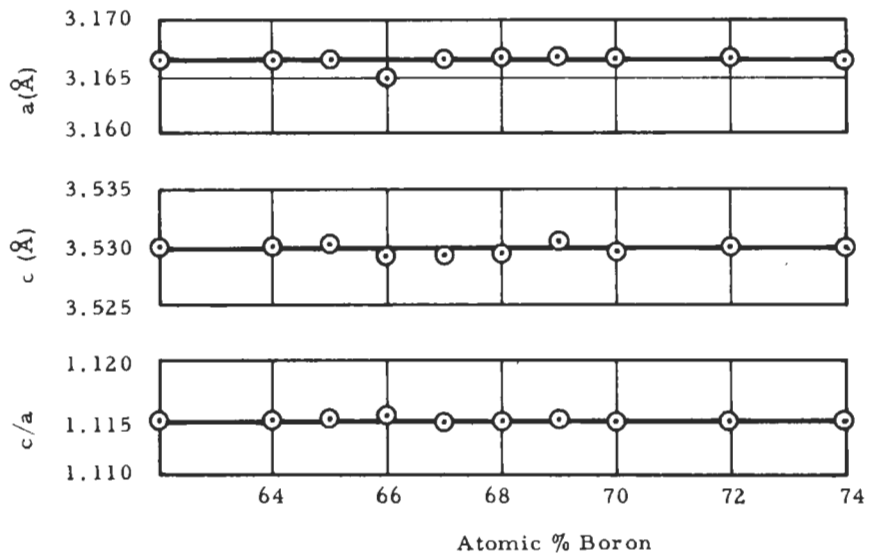


Figure 12. Lattice Parameters of Zirconium Diboride as a Function of the Boron Content.

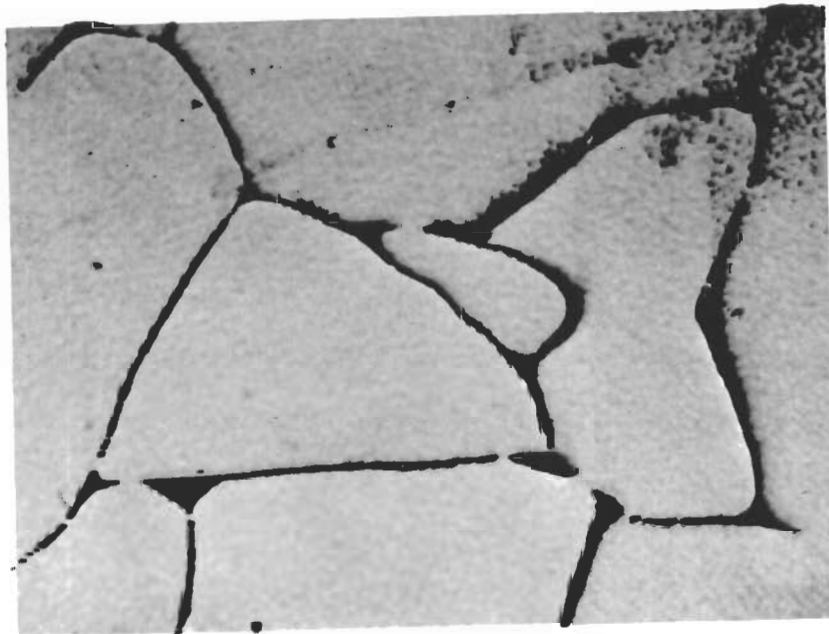


Figure 13. Zr-B (64.4 At% B), Quenched from 2000°C. Zirconium Diboride with Metal Phase at the Grain Boundaries.

X1000

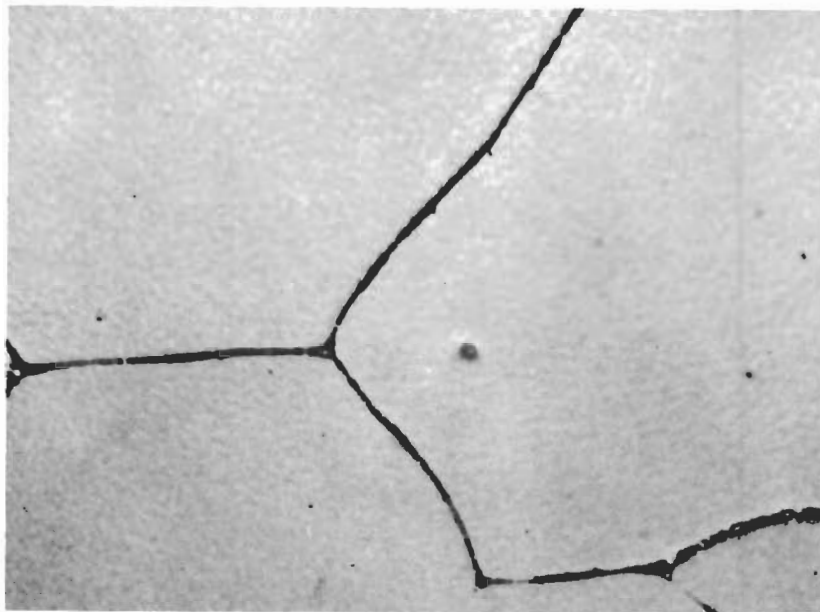


Figure 14. Zr-B (65.4 At% B), Quenched from 2600°C. X1000
ZrB₂, and Small Amounts of Grain-Boundary Zirconium.

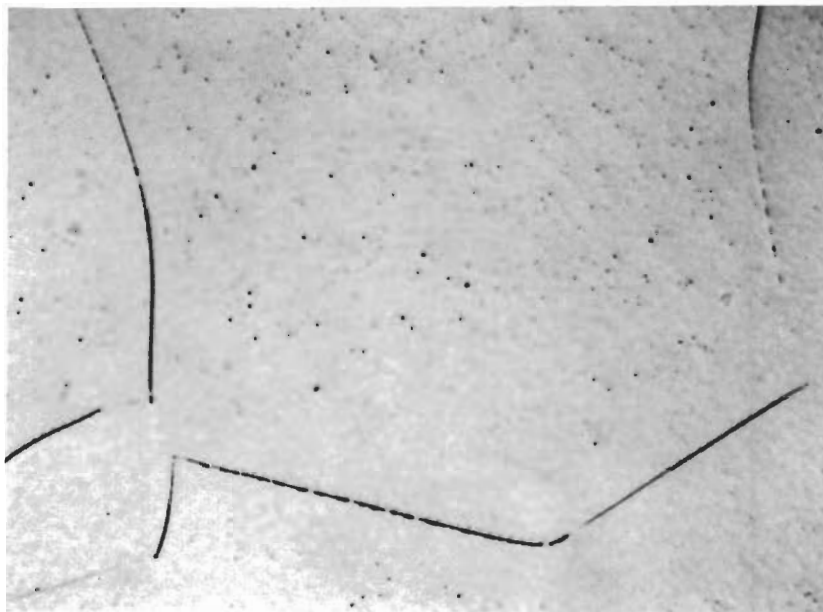


Figure 15. Zr-B (65.8 At% B), Quenched from 3000°C. X850
Low-Boron Boundary of ZrB₂; Minute Traces of
Second Phase Zirconium are Still Visible at the Grain
Boundaries.

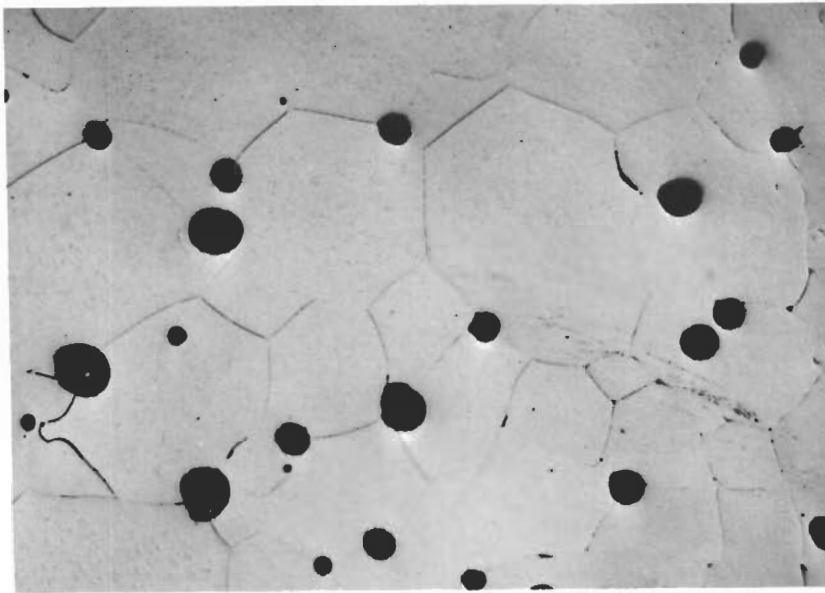


Figure 16. Zr-B (66.2 At% B), Quenched from 3245°C. X275
Single Phase ZrB₂. Pores (Black).

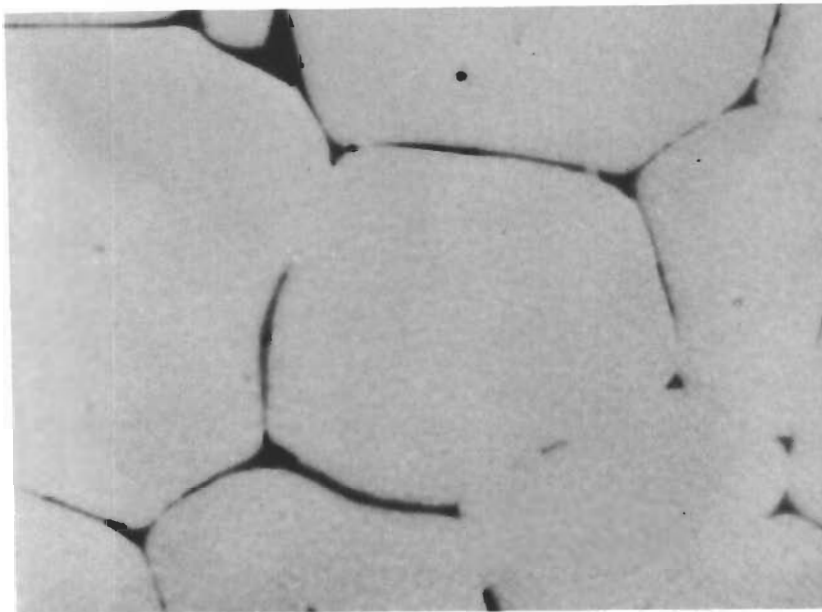


Figure 17. Zr-B (68.3 At% B), Quenched from 2700°C. X1000
ZrB₂, and Grain Boundary Boron.

diboride to be limited to composition close to stoichiometry (Figures 13 through 17). In neither case were precipitations noticed, which would indicate temperature-dependent phase boundaries.

4. Boron-Rich Equilibria

X-ray investigations on alloys with boron concentrations above 73 atomic percent which were heat-treated and quenched from temperatures above 1800°C, showed increasing amounts of dodecaboride. The average lattice parameters measured were $a = 7.408 \pm 0.002 \text{ \AA}$. The dodecaboride was present in small quantities only after quenching from above 2300°C, but its relative amount increased rapidly upon re-equilibration and quenching of the alloys at temperatures between 1800 and 2200°C; ZrB_{12} was obtained in almost pure form in the sample which had a nominal boron content of 90 atomic percent and could not be detected in alloys which were heat-treated and quenched from temperatures below 1700°C; it was not observed in furnace-cooled specimens after equilibration treatments in the vicinity of 2000°C.

The melting point measurements on high-boron (>80 At%) posed some problems, since the electrical conductivity of these alloys at temperature below approximately 1200°C was too poor to be measured with the ordinary Pirani technique; higher voltages applied across the sample at start-up proved to be unsatisfactory because of uncontrollable run-away effects. The difficulties were finally overcome by radiation-heating the samples to approximately 1500°C with the aid of a resistively heated tantalum strip. Above these temperatures the conductivities of the samples proved to be sufficiently high for self-resistance heating.

Although the melting point measurements on the high-boron alloys were not comparable in accuracy to the metal-rich alloys, they do indicate, that the dodecaboride melts incongruently (Table 4 and Figure 7).

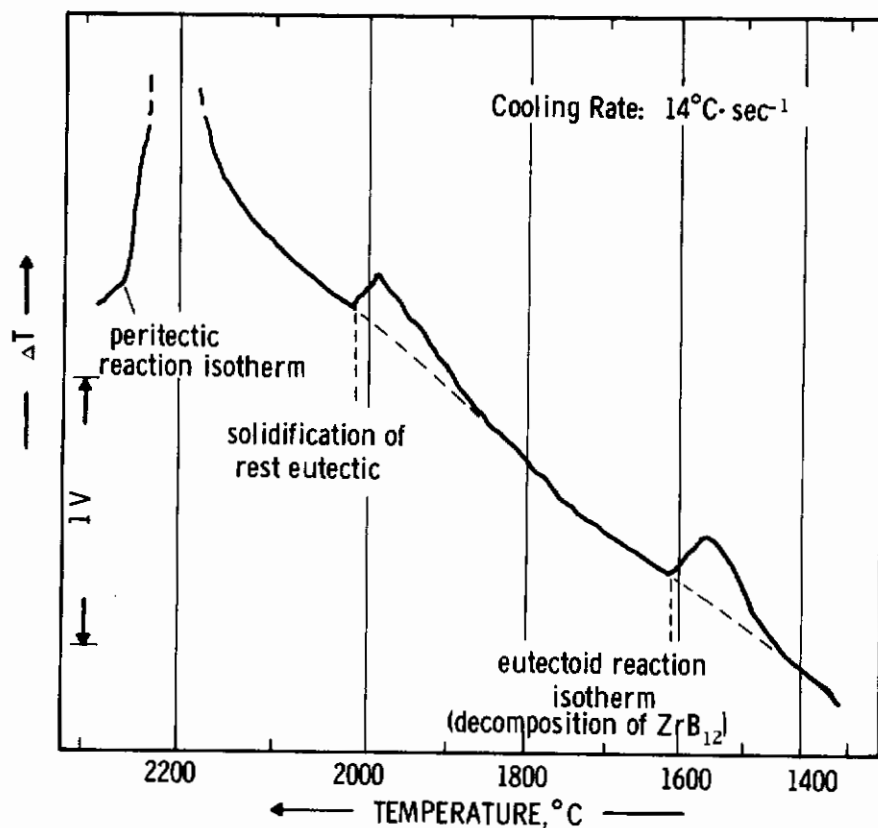


Figure 18. DTA-Thermogram (Cooling) of a Zirconium-Boron Alloy with 80 Atomic Percent Boron.

Note Appearance of the Eutectic $\text{ZrB}_{12} + \text{B}$ due to Incomplete Peritectic Reaction.

In favor of this interpretation are also the DTA-results (Figure 18), which showed reproducible thermal arrests at $\sim 2250^{\circ}\text{C}$ and 2000°C , the latter being associated with the solidification of the $\text{ZrB}_{12} + \text{B}$ eutectic.

The dodecaboride decomposes at temperatures around 1700°C into diboride and elemental boron (Figures 18, 19, and 20). The

reaction is strongly rate-dependent, as evidenced by the DTA-thermograms, and decomposition was generally found to be incomplete at cooling rates above 30°C per minute. Initiation of the decomposition reaction, however, occurs comparatively fast, and usually could not be prevented in experiments employing cooling speeds up to 80°C per second.

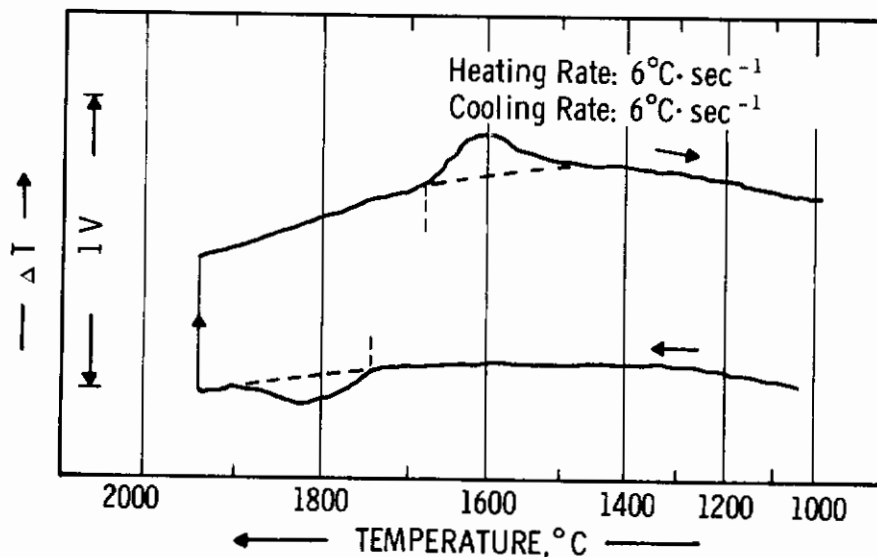


Figure 19. DTA-Thermogram of the Alloy from Figure 18 (80 At% B) at Lower Heating and Cooling Rates.

Note Shift of Apparent Eutectoid Temperatures on the Heating and Cooling Cycle.

Metallographically, the dodecaboride can be very easily distinguished from the accompanying phases ZrB_2 and boron by its characteristic purplish-pink color. The results of the metallographic investigations, gained on a large number of melted as well as heat-treated and quenched samples, are in confirmation of the evidence gained independently by DTA as well as X-ray techniques. A collection of representative microstructures of alloys from this concentration range are shown in Figures (21 through 27).

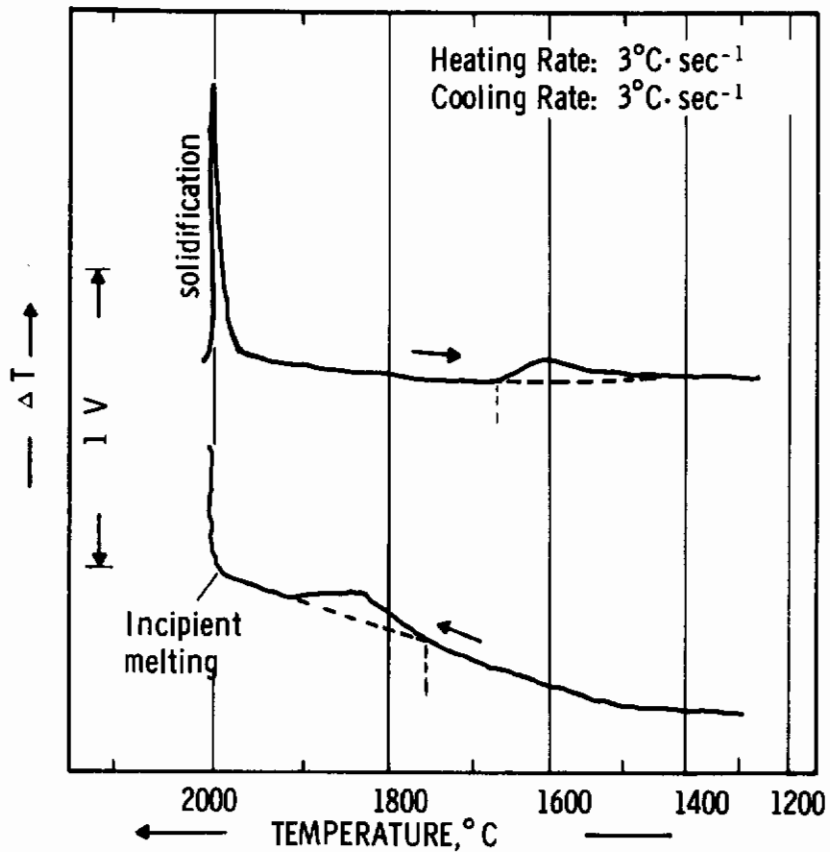


Figure 20. DTA-Thermogram of a Zirconium-Boron Alloy with 95 Atomic % Boron.

$\text{ZrB}_{12} + \text{B}$ Eutectic ($\sim 2000^{\circ}\text{C}$), and Formation (Heating) and Decomposition (Cooling) of the High Temperature Phase ZrB_{12} at $\sim 1700^{\circ}\text{C}$.

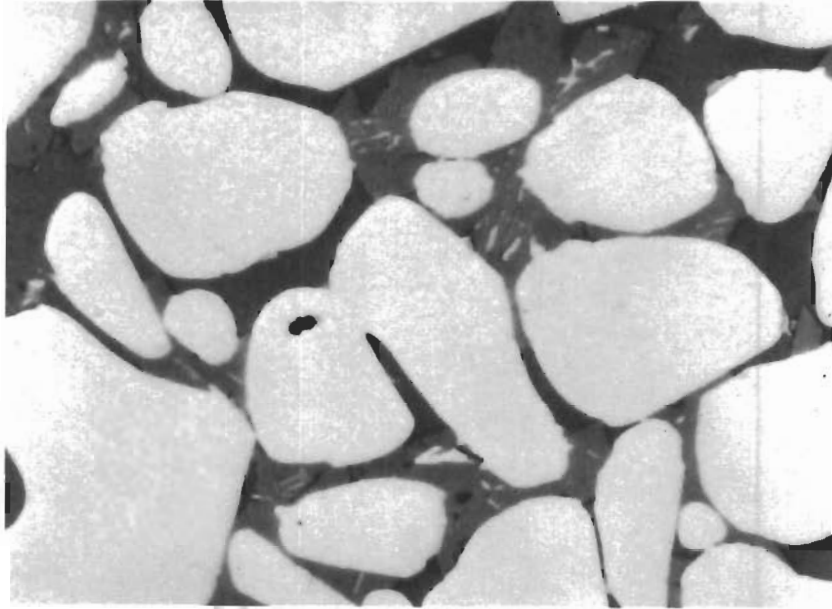


Figure 21. Zr-B (80 At% B), Cooled with Approximately 20°C per Second from 2280°C. X950
Primary ZrB_2 (Light), ZrB_{12} , and Boron.

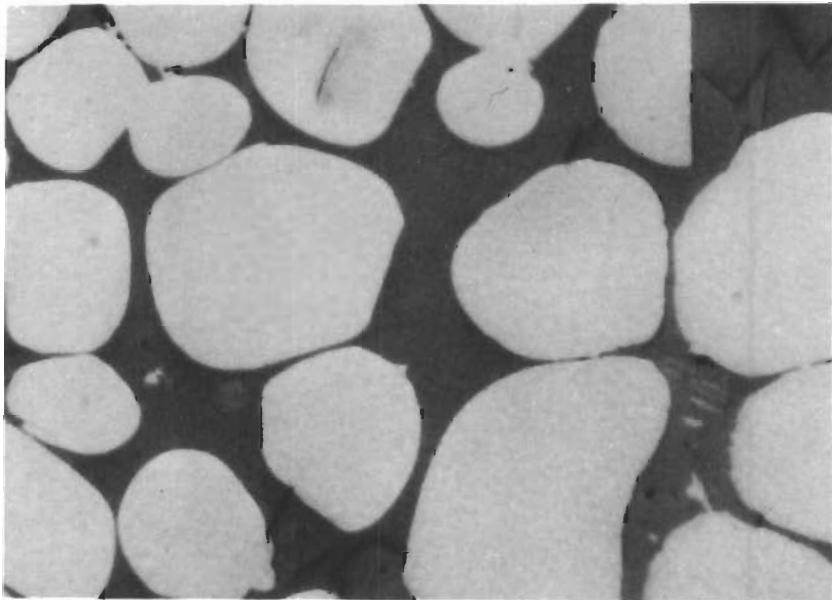


Figure 22. Zr-B (80 At% B), Partially Melted at 2280°C, X1000
Reannealed at 2200°C, and Quenched.
 ZrB_2 (Light), ZrB_{12} (Matrix), and Small Amounts of Boron.

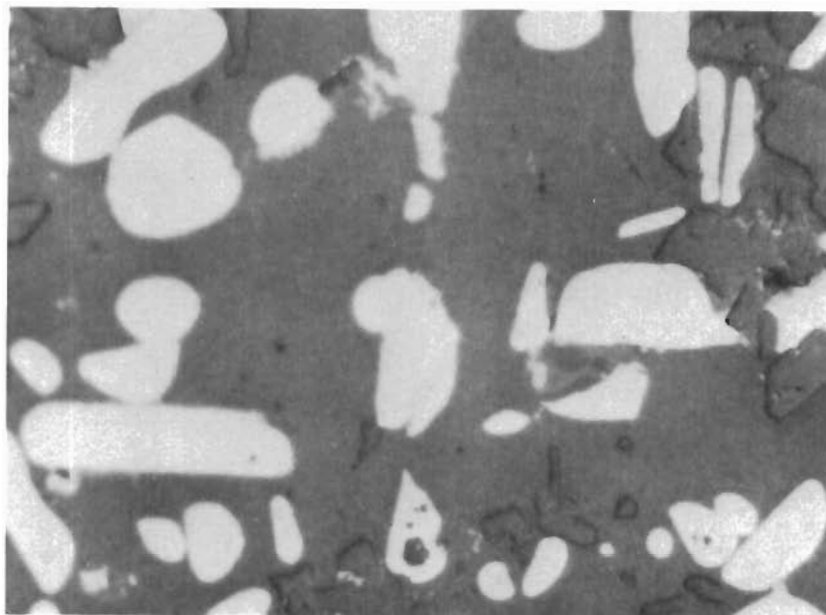


Figure 23. Zr-B (88 At% B), Melted, Re-equilibrated at 2200°C, and Quenched. X1000

ZrB₁₂ (Matrix), and Smaller Amounts of Uncombined ZrB₂ (Light) and Boron.

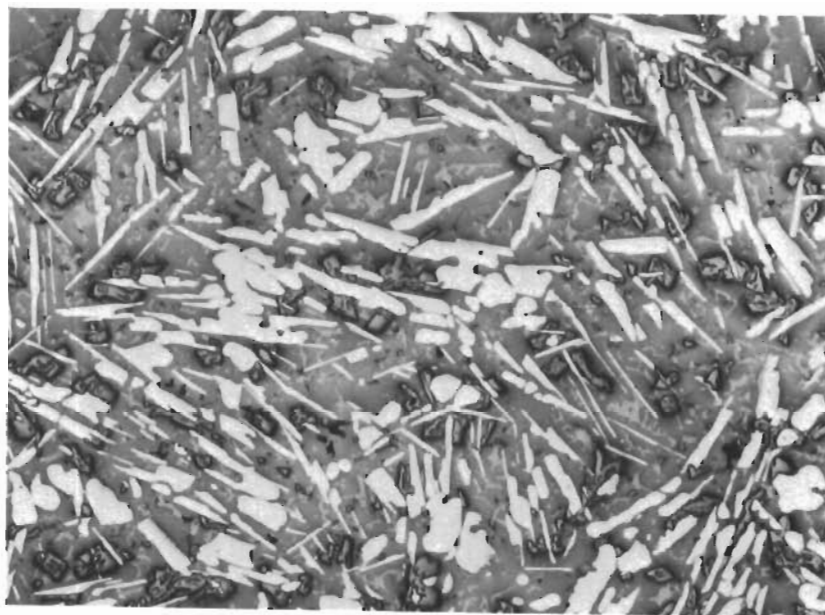


Figure 24. Zr-B (90 At% B), Cooled with $\sim 10^{\circ}\text{C}$ per Second from 2300°C. X130

Peritectic Reaction Mixture ZrB₂ + B + ZrB₁₂



Figure 25. Zr-B (90 At% B), Alloy from Figure 24
Re-equilibrated for 1/2 Hour at 2200°C,
and Quenched.

X1000

ZrB₁₂ with Small Amounts of Unreacted Zirconium
Diboride and Boron.

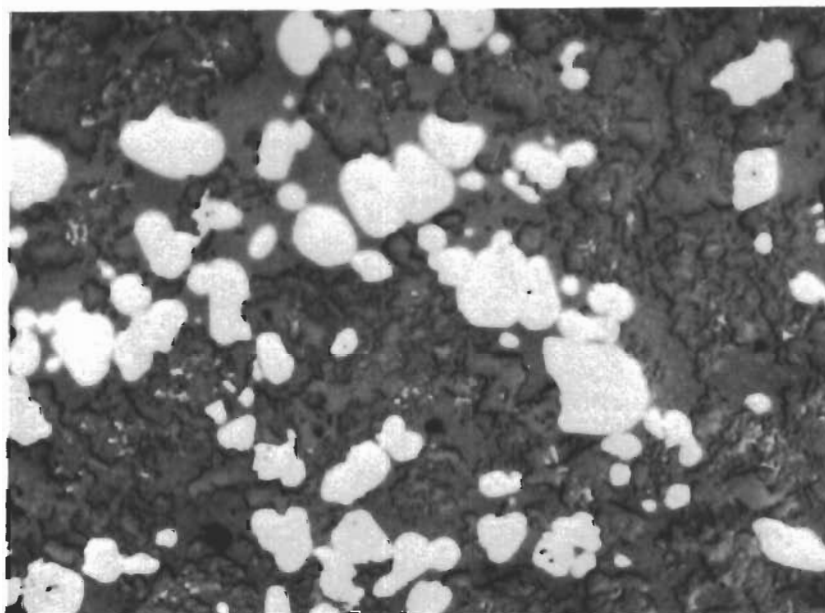


Figure 26. Zr-B (87 At% B), Melted, Re-equilibrated at
2200°C, and Cooled with 2°C per Second.

X1000

ZrB₂ with Partially Decomposed ZrB₁₂.

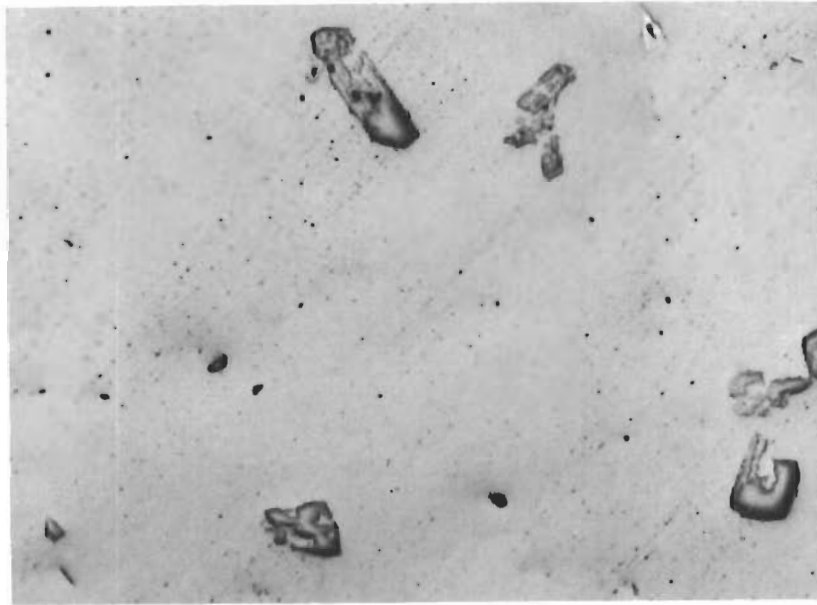


Figure 27. Zr-B (99 At% B), Cooled with Approximately 10°C per Second from 2100°C. X250
Boron with Isolated Grains of ZrB₁₂.

IV. DISCUSSION

The newly established phase relationships in the zirconium-boron system differ in a number of respects from the presently accepted diagram (Figure 2). Eutectic melting in the very metal-rich region occurs approximately 100°C lower than previously reported, and we also find the eutectic composition located somewhat closer to the metal phase. From the present investigations, it appears now firmly established, that no monoboride, at least not at temperatures above 1300°C, is formed in this alloy system, and that the earlier claimed face-centered cubic monoboride corresponded to an (C, O, N,)-stabilized impurity phase.

For the congruent melting point of ZrB₂ we measured 3245°C, which is approximately 200°C higher than values reported by C. Agte (2990°C),

Contrails

K. Moers (3040°C) and F. W. Glaser (3040°C). These differences are not surprising, since the homogeneity range of the diboride is very narrow, and small deviations, say 0.5 to 1 atomic percent, from the congruently melting composition, already results in considerable lower values (Figure 7). Since even in careful experimentations, the composition reproducibility is never better than ± 0.2 atomic percent, it usually requires a large number of closely-spaced alloys to ascertain, that in the experimentations the congruently melting composition had been included.

In the boron-rich region, our diagram differs from that proposed by W. Schedler⁽⁸⁾ and F. W. Glaser and B. Post⁽³⁾ (Figure 2) in that we find incongruent melting for the dodecaboride rather than maximum melting at temperatures around 2700°C, as proposed by these authors. Unambiguous assessment of their data however, is difficult. Their melting experiments were carried out in graphite containers, which would initially lead one to suspect, that the temperatures reported would more closely refer to those of the ternary or quasibinary eutectica formed in the alloy system Zr-B-C. Experiments, carried out in the boron corner of the ternary systems, however, proved this assumption to be only conditionally acceptable. The maximum solidus temperatures in the concentration area $ZrB_{12}-B_4C-B$ are limited to temperatures below 2000°C, rising to approximately 2200 to 2300°C in the field $ZrB_2-ZrB_{12}-B_4C$. The highest solidus temperatures, approximately 2400°C, were measured on quasibinary alloys ZrB_2-B_4C . This temperature, however, is still 260°C lower than the reported melting point for ZrB_{12} . In either instance, we observed rapid interaction between high-boron alloys and graphite to occur above solidus, which limits the observable melting temperatures essentially to those of the corresponding quasibinary or ternary eutectica. In view of this latter finding, the high melting point measured for ZrB_{12} remains surprising.

REFERENCES

- 1 B. Post and W. Glaser: J. Chem. Phys. 20 (1952), 1050.
- 2 F. W. Glaser: Trans. AIME 194 (1952), 391
- 3 F. W. Glaser and B. Post: Trans. AIME 197 (1953), 1117.
- 4 E. Rudy and F. Benesovsky: Mh. Chem. 92 (1961), 415.
- 5 P.M. McKenna: Ind. Eng. Chem. 28 (1936), 767.
- 6 R. Kiessling: Acta Chem. Scand. 3 (1949), 90.
- 7 L. Brewer, D.L. Sawyer, D.H. Templeton, and C.H. Dauben: J. Am. Ceram. Soc. 34 (1951), 173.
- 8 W. Schedler: Thesis, Technische Hochschule graz, Austria (1951).
- 9 V.A. Eplebaum and M.A. Gurewitsch: Zhur.Fiz.Chim. 31 (1957), 708.
- 10 K. Moers: Z. anorg. allg. Chemie 198 (1931), 262.
- 11 C. Agte: Thesis, Technische Hochschule Berlin, 1931.
- 12 P. Schwarzkopf and F.W. Glaser: Z. Metallkde 44 (1953), 353.
- 13 J.T. Norton, H. Blumenthal, and S.J. Sindeband: Trans AIME 185 (1949), 749.
- 14 C.T. Baroch and T.E. Evans: J. Metals 7 (1955), 908.
- 15 W. Zachariasen: Acta Cryst. 2 (1949), 94.
- 16 E. Rudy, St. Windisch, and Y.A. Chang: AFML-TR-65-2, Part I, Vol. I (January 1965).
- 17 H.D. Heetderks, E. Rudy, and T. Eckert: AFML-TR-65-2, Part III, Volume I (May 1965).
- 18 E. Rudy and St. Windisch: AFML-TR-65-2, Part I, Vol. VII (Oct 1965).
- 19 E. Rudy, D.P. Harmon, and C.E. Brukl: AFML-TR-65-2, Part I, Volume II (May 1965).
- 20 A more detailed treatment of the phase conditions will be presented in the discussion of the Zr-B-C System (AFML-TR-65-2, Part II, to be published).

DOCUMENT CONTROL DATA - R&D

(Security classification of title, body of abstract and indexing annotation must be entered when the overall report is classified)

1. ORIGINATING ACTIVITY (Corporate author) Aerojet-General Corporation Materials Research Laboratory Sacramento, California		2a. REPORT SECURITY CLASSIFICATION Unclassified	
		2b. GROUP N.A.	
3. REPORT TITLE Ternary Phase Equilibria in Transition Metal-Boron-Carbon-Silicon Systems Part I. Related Binary Systems. Volume VIII, Zr-B System			
4. DESCRIPTIVE NOTES (Type of report and inclusive dates)			
5. AUTHOR(S) (Last name, first name, initial) E. Rudy St. Windisch			
6. REPORT DATE January 1966		7a. TOTAL NO. OF PAGES 34	7b. NO. OF REFS 20
8a. CONTRACT OR GRANT NO. AF 33(615)-1249		9a. ORIGINATOR'S REPORT NUMBER(S) AFML-TR-65-2 Part I, Vol. VIII	
b. PROJECT NO. 7350			
c. Task No. 735001		9b. OTHER REPORT NO(S) (Any other numbers that may be assigned this report) N.A.	
d.			
10. AVAILABILITY/LIMITATION NOTICES This document is subject to special export controls and each transmittal to foreign governments or foreign nationals may be made only with prior approval of the Metals & Ceramics Div. (MAM), AF Laboratory, WPAFB, Ohio.			
11. SUPPLEMENTARY NOTES 2		12. SPONSORING MILITARY ACTIVITY AFML (MAMC) Wright-Patterson AFB, Ohio 45433	
13. ABSTRACT The binary alloy system zirconium-boron has been investigated by means of X-ray, metallographic, melting point, and differential-thermoanalytical techniques. The experimental alloy material comprised of hot-pressed and heat-treated, arc- and electron-beam melted, as well as equilibrated and quenched alloy material. All phases of the experimental investigations were supported by chemical analysis. The results of the present investigation, which resulted in the establishment of a complete phase diagram for the system, are discussed and compared with previously established system data. <i>This document has been approved for public release and sale; its distribution is unlimited.</i>			

14. KEY WORDS	LINK A		LINK B		LINK C	
	ROLE	WT	ROLE	WT	ROLE	WT
Binary Boride Phase Equilibria Zirconium-Boron						

INSTRUCTIONS

1. **ORIGINATING ACTIVITY:** Enter the name and address of the contractor, subcontractor, grantee, Department of Defense activity or other organization (*corporate author*) issuing the report.
- 2a. **REPORT SECURITY CLASSIFICATION:** Enter the overall security classification of the report. Indicate whether "Restricted Data" is included. Marking is to be in accordance with appropriate security regulations.
- 2b. **GROUP:** Automatic downgrading is specified in DoD Directive 5200.10 and Armed Forces Industrial Manual. Enter the group number. Also, when applicable, show that optional markings have been used for Group 3 and Group 4 as authorized.
3. **REPORT TITLE:** Enter the complete report title in all capital letters. Titles in all cases should be unclassified. If a meaningful title cannot be selected without classification, show title classification in all capitals in parenthesis immediately following the title.
4. **DESCRIPTIVE NOTES:** If appropriate, enter the type of report, e.g., interim, progress, summary, annual, or final. Give the inclusive dates when a specific reporting period is covered.
5. **AUTHOR(S):** Enter the name(s) of author(s) as shown on or in the report. Enter last name, first name, middle initial. If military, show rank and branch of service. The name of the principal author is an absolute minimum requirement.
6. **REPORT DATE:** Enter the date of the report as day, month, year; or month, year. If more than one date appears on the report, use date of publication.
- 7a. **TOTAL NUMBER OF PAGES:** The total page count should follow normal pagination procedures, i.e., enter the number of pages containing information.
- 7b. **NUMBER OF REFERENCES:** Enter the total number of references cited in the report.
- 8a. **CONTRACT OR GRANT NUMBER:** If appropriate, enter the applicable number of the contract or grant under which the report was written.
- 8b, 8c, & 8d. **PROJECT NUMBER:** Enter the appropriate military department identification, such as project number, subproject number, system numbers, task number, etc.
- 9a. **ORIGINATOR'S REPORT NUMBER(S):** Enter the official report number by which the document will be identified and controlled by the originating activity. This number must be unique to this report.
- 9b. **OTHER REPORT NUMBER(S):** If the report has been assigned any other report numbers (*either by the originator or by the sponsor*), also enter this number(s).
10. **AVAILABILITY/LIMITATION NOTICES:** Enter any limitations on further dissemination of the report, other than those

imposed by security classification, using standard statements such as:

- (1) "Qualified requesters may obtain copies of this report from DDC."
- (2) "Foreign announcement and dissemination of this report by DDC is not authorized."
- (3) "U. S. Government agencies may obtain copies of this report directly from DDC. Other qualified DDC users shall request through _____."
- (4) "U. S. military agencies may obtain copies of this report directly from DDC. Other qualified users shall request through _____."
- (5) "All distribution of this report is controlled. Qualified DDC users shall request through _____."

If the report has been furnished to the Office of Technical Services, Department of Commerce, for sale to the public, indicate this fact and enter the price, if known.

11. **SUPPLEMENTARY NOTES:** Use for additional explanatory notes.
12. **SPONSORING MILITARY ACTIVITY:** Enter the name of the departmental project office or laboratory sponsoring (*paying for*) the research and development. Include address.
13. **ABSTRACT:** Enter an abstract giving a brief and factual summary of the document indicative of the report, even though it may also appear elsewhere in the body of the technical report. If additional space is required, a continuation sheet shall be attached.

It is highly desirable that the abstract of classified reports be unclassified. Each paragraph of the abstract shall end with an indication of the military security classification of the information in the paragraph, represented as (TS), (S), (C), or (U).

There is no limitation on the length of the abstract. However, the suggested length is from 150 to 225 words.

14. **KEY WORDS:** Key words are technically meaningful terms or short phrases that characterize a report and may be used as index entries for cataloging the report. Key words must be selected so that no security classification is required. Identifiers, such as equipment model designation, trade name, military project code name, geographic location, may be used as key words but will be followed by an indication of technical context. The assignment of links, rules, and weights is optional.